Evaluation of measurement technique for a precision aspheric artefact using a nano-measuring machine

Xiaomei Chen, Andrew Longstaff, Simon Fletcher, Alan Myers
University of Huddersfield, Queensgate, Huddersfield HD1 3DH, UK

Abstract

A precision aspheric artefact is measured in 3D by a commercially available nano-measuring machine (NMM) integrated with a contact inductive sensor as the probe. The mathematics of 3D compensation of the error caused by the probe radius is derived. The influence of the probe radius measurement uncertainty on the compensation errors for the 3D measurements is discussed. If the calibration uncertainty of probe radius is 1μm and 0.1 μm respectively, the compensation errors for a paraboloid artefact are within 100 nm and 10 nm respectively, and the artefact measurement uncertainties are 103 nm and 26 nm respectively. The artefact calibration uncertainty depends more on the uncertainty of the probe radius calibration than the probe radius.

1 Introduction

Traditionally, rotationally-symmetrical aspheric surfaces with small dimensions and nano scale accuracy are measured by an optical interferometry microscope [1,2]. However, they are measured more and more by the coordinate-measuring machines (CMM) in different configurations and mechanical schemes [3-5], especially when it comes to the calibration of standard artefacts, such as a high precision traceable freeform reference standard developed in National Physics Laboratory (NPL) [6]. As described by the previous paper [7], a precision rotationally-symmetrical aspheric artefact has been 3D-measured by a commercially available nano-measuring machine (NMM) [8] with a measuring volume of 25 mm × 25 mm × 5 mm. In this device, three homodyne laser interferometers are employed for the

measurement of the displacement and servo control of the motion stage along the *x*-, *y*- and *z*-axis. In its configuration, the measurement probe mounted on the metrology frame is located at the intersection point of three measurement laser beams of interferometers, therefore the Abbe error which is a dominant error source in dimensional metrology could be minimised. A cost-effective contact inductive sensor (CIS) (TESA GT22) with high resolution, and relatively wide measuring range has been mechanically and electrically integrated on the top of the NMM as the probe for the purpose of calibrating the artefacts with rotationally-symmetrical form, non-rotationally-symmetrical aspheric form as well as freeform. The inductive sensor has ±2 mm measuring range, 10 nm resolution, 1.5 mm nominal probe radius and 0.16 N measuring forces.

2 A paraboloid artefact and NMM integrated with a CIS

The NMM integrated with a CIS aforementioned is shown in figure 1. As a good example that the CIS-integrated NMM is employed for the calibration of an aspheric artefact, a single-point, diamond-turned, precision concave paraboloid artefact, shown on the *x*-*y*-*z* measurement table of NMM in figure 1, with a diameter of 22mm, chord length of 3mm, surface roughness *R*a of 5nm has been 3D-measured. Because a rotationally- symmetrical paraboloid can be mathematically expressed by a simple mathematic function, it is manufactured with the intended use of calibrating ultra-precision machine tools or form measurement instruments such as stylus profilers after it is metrological-traceably calibrated.

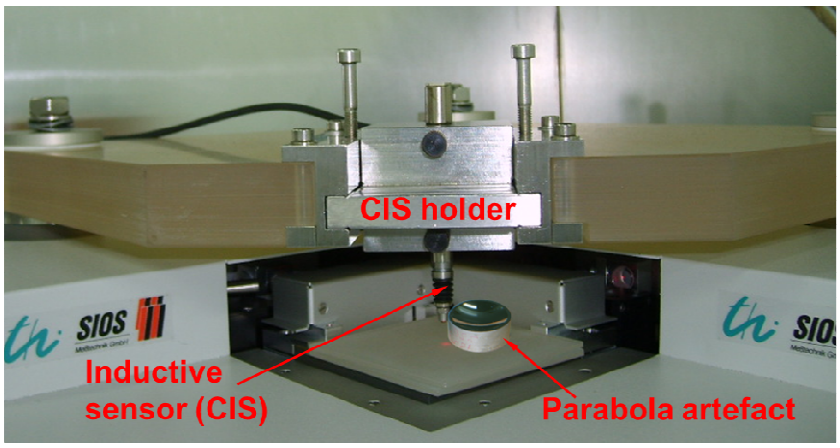

Figure 1: A precision concave paraboloid artefact, processed by a single-point diamond-turning machine is measured by NMM integrated with a CIS as probe.

The general non-rotationally-paraboloid artefact is mathematically expressed by

$$f(x, y) = ax^2 + by^2 + cx + dy + e \quad (1)$$

For the rotationally-symmetrical paraboloid artefact, the nominal coefficients of the binomial term for the paraboloid of rotation: $a = b = 3/121$ (≈ 0.0248), and the nominal coefficients of the monomial term and constant term: $c, d, e = 0$ in the coordinate system of the diamond-turning machine, and $c, d, e \neq 0$ in the coordinate system of such a measuring instruments as the NMM. A least-square-fitting process was used to determine the coefficients ***a***, ***b***, ***c***, ***d*** and ***e*** by using 3D coordinate data measured by the NMM.

Since the intersection between the rotational-paraboloid and any plane that is parallel to z-axis is a parabola mathematically, as a comparison to see the influence of the probe radius, the artefact has also been measured in 2D by a stylus profiler with a 10μm stylus radius – though in metrology it cannot be directly traced back to SI length unit. A least-square-fitting method was also used to determine coefficient ***a***. When the 3D- and 2D-fitting results were compared to the nominal value ***a***, it were found that the 2D-fitting results were closer to the nominal coefficients than 3D-fitting results. The probe radius is a cause of this, and it needs to be compensated. Therefore, in this paper, the probe radius-caused error is compensated and the influence of probe radius measurement uncertainty on the compensation errors for the paraboloid artefact is discussed in this paper.

3 Mathematics of 3D compensation of probe radius

Although mathematics of the 3D compensation for probe radius-caused error were derived in references [8,9], a concise, immediate and complete derivation is presented as follows.

If a curved surface implicitly expressed by $F(x,y,z)=0$ has the continuous partial differentiations $F_x(x_0,y_0,z_0)$, $F_y(x_0,y_0,z_0)$ and $F_z(x_0,y_0,z_0)$ at a point (x_0,y_0,z_0), the normal vector at this point is

$$n = (F_x(x_o, y_o, z_o), F_y(x_o, y_o, z_o), F_z(x_o, y_o, z_o)) \quad (2)$$

For curved surface explicitly expressed by $z = f(x, y)$, to set $F(x,y,z) = f(x, y) - z$, $F_x(x,y,z) = f_x(x,y)$, $F_y(x,y,z) = f_y(x,y)$ and $F_z(x,y,z) = -1$. Therefore, if the partial differentiations $f_x(x,y)$ and $f_y(x,y)$ of function $f(x,y)$ is continuous at a point $p(x, y, z)$, the normal vector at this point is

$$n = (f_x(x, y), f_y(x, y), -1) \quad (3)$$

Now $z = f(x, y)$ is the fitted curved surface from the measured coordinate data $p(x_i, y_i, z_i)$ (i=1, 2, 3, ⋯, n) of a series of the spherical probe centres with radius ***r*** as shown by figure 2. In order to see clearly the geometrical relationship between the probe sphere and the paraboid surface, only half-sectioned paraboloid and probe sphere are drawn in figure 2, where $\boldsymbol{p_E}$ is the

actual contact point between a probe and a curved surface, Δz_i is probe radius-caused error. The enveloped curved surface of the probe sphere, with equidistance $\boldsymbol{r}$ from $z = f(x, y)$, can be express as

$$f_E(x,y) = f(x,y) - r \cdot \vec{n} \tag{4}$$

where, $\vec{n}$ is the normal vector of the curved surface $z = f(x, y)$ at point $\boldsymbol{p}$.

The cosine of the angle between the normal vector and z-axis direction is

$$\cos\gamma = \frac{1}{\sqrt{f_x^{\,2}(x,y) + f_y^{\,2}(x,y) + 1}} \tag{5}$$

Equation (4) can be rewritten as

$$f_E(x,y) \approx f(x,y) - r/\cos\gamma \tag{6}$$

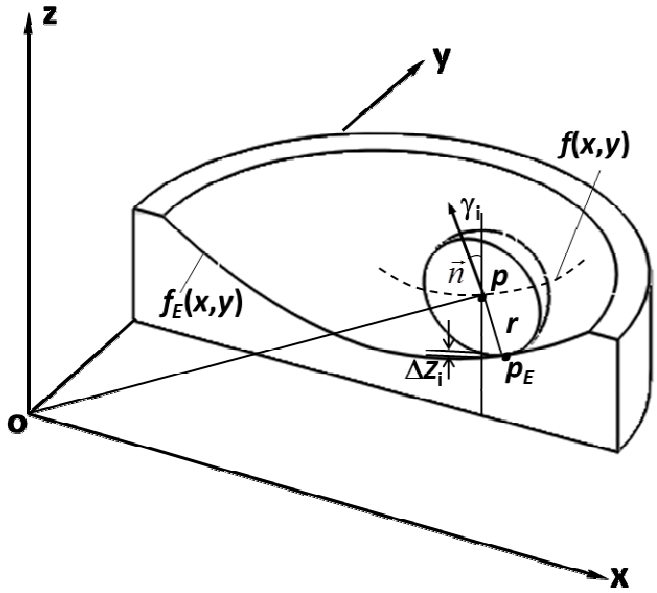

Figure 2: schematic of probing error caused by probe radius

The measurement errors caused by the spherical probe radius are

$$\Delta z_i = f(x_i, y_i) - f_E(x_i, y_i) - r \approx r(1/\cos\gamma_i - 1)\ (i = 1, 2, 3\cdots, n) \tag{7}$$

After compensation, the coordinate data are

$$f_E(x_i, y_i) = f(x_i, y_i) - \Delta z_i = f(x_i, y_i) - r(1/\cos\gamma_i - 1)\ \ (i = 1, 2, 3\cdots, n) \tag{8}$$

For the fitted paraboloid surface mathematically expressed by equation (1), the partial differentiations at a point (x_i, y_i, z_i) are respectively

$$\begin{cases} f_x(x_i, y_i) = 2ax_i + c \\ f_y(x_i, y_i) = 2by_i + d \end{cases} \tag{9}$$

and

$$\cos\gamma_i = \frac{1}{\sqrt{(2ax_i + c)^2 + (2by_i + d)^2 + 1}} \tag{10}$$

After compensation, coordinate data are

$$f_E(x_i, y_i) = f(x_i, y_i) - r \cdot (\sqrt{(2ax_i + c)^2 + (2by_i + d)^2 + 1} - 1) \ (i = 1, 2, 3 \cdots, n) \tag{11}$$

Therefore, the newly fitted paraboloid surface from the compensated coordinate data is

$$f_E(x, y) = Ax^2 + By^2 + Cx + Dy + E \tag{12}$$

Before and after the compensation of probe radius, the fitting errors are respectively

$$\delta = \sum_{i=1}^{n} \left| z_i - (ax_i^2 + by_i^2 + cx_i + dy_i + e) \right| \tag{13}$$

and

$$\delta = \sum_{i=1}^{n} \left| f_E(x_i, y_i) - (Ax_i^2 + By_i^2 + Cx_i + Dy_i + E) \right| \tag{14}$$

4 Experiments and results

4.1 Fitting experiments

The fitted paraboloid coefficients from the data measured by NMM and the fitted parabola coefficients from the data measured by a stylus profiler, as a comparison, are all listed in table 1, where the CIS probe radius and stylus radius are 1.4mm and 10 μm respectively.

Table 1: paraboloid coefficients fitted from 3D and 2D data measured by NMM and stylus profiler respectively

		Before compensation		After compensation	
Measuring instruments		NMM	profiler	NMM	profiler
Coefficients	*a*	0.0267	0.0248	0.0248	0.0248
	b	0.0266	−	0.0248	−
	c	-0.6034	-0.2548	-0.5612	-0.2548
	d	-0.4835	−	-0.4497	−
	e	4.0771	0.2478	3.6847	0.2475
Fitting error δ(μm)		4.3	0.24	0.1	2.3×10^{-5}

As was expected, for NMM measurement, the fitted coefficients ***a, b*** are greater than the nominal ones before the compensation, and the fitted coefficients ***A*** and ***B*** are as the same values as the nominal ones after the compensation; for stylus profiler measurement, the fitted coefficients ***a, b*** before the compensation and ***A***, ***B*** after the compensation hardly change because the stylus radius is small enough to be neglected. The fitting errors reduce by half after the compensation for both NMM and stylus profiler measurements.

The fitted paraboloids from the NMM measurement data, before and after the compensation of the probe radius-induced errors, are shown in figure 3.

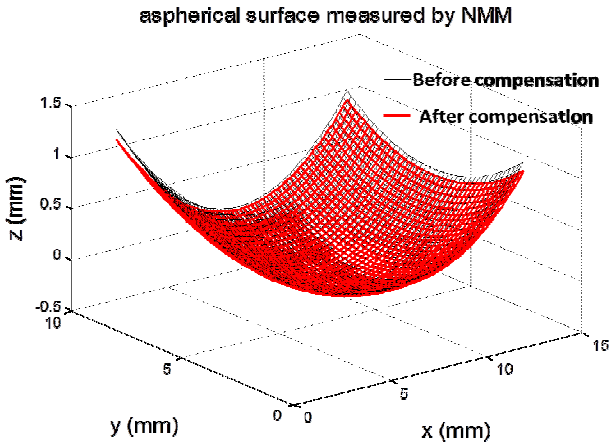

Figure 3: Paraboloids before and after 3D compensation of probe radius-caused errors if probe radius r =1.4mm.

4.2 Compensation error caused by uncertainty of probe radius

By differentiating equation (11) with respect to ***r***, the compensation uncertainty caused by the measurement uncertainty of the probe radius is

$$u_c(\Delta z_i) = (\sqrt{(2ax_i + c)^2 + (2by_i + d)^2 + 1} - 1) \cdot u_c(r) \qquad (15)$$

If the measurement uncertainty of the probe radius is $u_c(r)$ = 1μm and $u_c(r)$ = 0.1μm respectively, the maximum of compensation errors $u_c(\Delta z_i)$ are 100 nm and 10 nm respectively for the measured artefact. Here only the compensation errors, corresponding to the measurement uncertainty of 100 nm are drawn in figure 4.

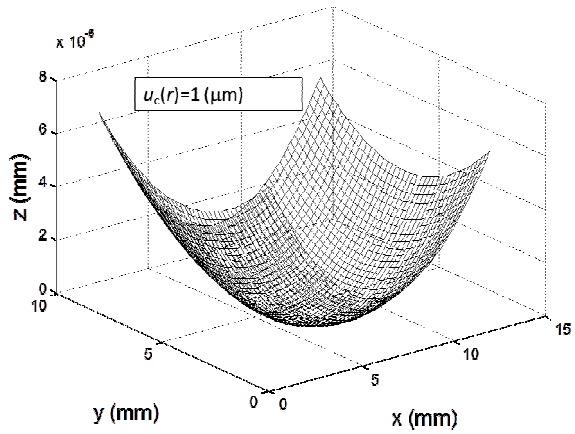

Figure 4: Compensation error caused by 1μm uncertainty of probe radius.

4.3 Artefact measurement uncertainty

According to the analysis of measurement uncertainty in the previous paper [7], when integrated with a CIS as probing sensor whose measurement repeatability is 10 nm, standard measurement uncertainty of the NMM for the spatial measurement volume of $l_x \times l_y \times l_z$ is

$$u_c(l) = (17.5 + 0.218l) \text{ (nm)} \tag{16}$$

where $l = (l_x^2 + l_y^2 + l_z^2)^{\frac{1}{2}}$, and its unit is millimetre.

Considering the compensation uncertainty $u_c(\Delta z)$ caused by the measurement uncertainty of a probe radius, for the measurement of a coordinate point p (x, y, z) on the surface of an aspheric artefact, the measurement uncertainty is

$$u_c(p) = [u_c^2(l) + u_c^2(\Delta z)]^{\frac{1}{2}} \tag{17}$$

Since the volume of paraboloid artefact is 22 mm × 22 mm × 4 mm and l ≈ 31.5 mm, $u_c(l)$ = 24 nm. If $u_c(\Delta z)$ = 100 nm, $u_c(p)$ ≈ 103 nm; if $u_c(\Delta z)$ = 10 nm, $u_c(p)$ ≈ 26 nm. Apparently, the artefact calibration uncertainty depends more on the uncertainty of the probe radius calibration than the probe radius.

5 Conclusion

An aspheric artefact has been successfully measured by a contact inductive sensor (CIS) that is integrated into the nano-measuring machine (NMM) as a probe. Ideally, the radius of a probe is as small as possible. However, for a cost effect probe, even with a relatively large radius when compared with the

10 μm radius of a stylus profiler, the probing error caused by its radius can be compensated. If the probe radius can be precisely calibrated beforehand with uncertainty of 1 μm and 0.1 μm respectively, the compensation errors caused by the probe radius uncertainty are within 100nm and 10 nm respectively for the measurement of the paraboloid artefact indicated in this paper, and the artefact measurement uncertainty is 103 nm and 26 nm respectively. It is concluded that the artefact measurement uncertainty depends more on the uncertainty of the probe radius calibration than on the probe radius itself.

Aacknowledgement

The authors gratefully acknowledge the UK's Engineering and Physical Sciences Research Council (EPSRC) funding of the EPSRC Centre for Innovative Manufacturing in Advanced Metrology (Grant Ref: EP/I033424/1).

References

[1]Küchel Michael F "Interferometric measurement of rotationally symmetric aspheric surfaces", http://www.zygo.com/library/papers/proc_TD04-25.pdf
[2]McBride W "The 3D measurement and analysis of aspheric surface" 2009, http://eprints.soton.ac.uk/65103/1/The_Measurement_and_Analysis_of_Aspheric_Surfaces.pdf
[3]Xiao Muzheng, Jujo satomi, Takahashi Satoru, Takamasu Kiyoshi "nanometer Profile measurement of large aspheric optical surface by scanning deflectometry with rotatable devices" Proc. SPIE 8126, Optical manufacturing and testing IX, 83260R, 2011
[4]Savio E, Chiffre L De"An artefect for traceable freeform measurements on coordinate measuring machines", Prec. Eng. Vol.26, 58-68, 2012
[5] Rens Henselmans "non-contact measurement machine for freeform optics", Doctoral thesis, 2009, http://alexandria.tue.nl/extra2/200910728.pdf
[6] http://www.npl.co.uk/upload/pdf/freeform-high-precision.pdf
[7]Chen Xiaomei, Wan Yu, Koenders Ludger and Schilling Meinhard "Measurements of dimensional standards and etalons with feature size from tens of micrometres to millimetres by using sensor strengthened nanomeasuring machine" **Measurement** Vol.43, 1369-1375, 2010.
[8]Jäger G, Hausotte T, Manske E, Büchner H-J, Mastylo R, Dorozhovets N and Hofmann N "Nanomeasuring and nanopositioning engineering". **Proc. SPIE** 6280, 628001, 2006.
[9]Lu Chunxia, Lao qicheng, Zhu Qiang and wang Jianhua "3D probe radius compensation in measurement of characterized curves of complex helicoidal surface", **IEEE** 2nd International conference on mechanical and electronics engineering (ICMEE 2010), V2, 127-130, 2010.
[10]Wang J, Lin Q and Qiao G "The trace surface of probe in measurement of complex surfaces and 3D probe compensation", **Acta Metrologica Sinica** V15,108-113, 1994.